Impedance Interferometry for Temperature Sensing in High-Stress, High-Temperature Applications

Zecheng Li, Nathanial Matz, Ravi Saraf, Joseph Turner, and Shubhendu Bhardwaj
University Of Nebraska-Lincoln, Lincoln, NE, USA.

***Abstract*—This paper presents a novel approach for monitoring and preventing overheating in wind turbine rollers using an integrated antenna system. A bimetallic strip embedded within the roller deforms in response to elevated temperatures, altering the reflection coefficient (S_{11}) of the coaxial cable. Simulations and experiments, including controlled heating tests conducted with a Vector Network Analyzer (VNA), demonstrate a strong correlation near 1.6 GHz. These results validate the feasibility of using the S_{11} signal for thermal anomaly detection. This approach paves the way for the development of RFID-based solutions to enhance the reliability and safety of wind turbines.**

I. Introduction

The challenges of overheating in wind turbine systems remain a critical engineering issue [1], driven by the complex interactions of thermal dynamics, mechanical components, and environmental factors. Effective thermal management is essential to enhance the reliability, efficiency, and service life of wind turbine operations. In recent years, accurate in situ prediction of roller temperatures has emerged as a significant engineering challenge [2]–[5]. Due to the mobile nature of the rollers and the high-stress operating environment, most existing solutions have relied on data-driven techniques and statistical models for temperature prediction.

This study investigates the feasibility of an RFID solution combined with a passive impedance measurement sensor to detect temperature variations (Fig. 1(b)). Local sensing within the roller is demonstrated. Although the ultimate goal is to develop a fully wireless solution, this work validates the efficacy of an impedance-based sensor tested using a coaxial cable connected to a Vector Network Analyzer (VNA). Simulations and experimental measurements confirm the viability of this method, laying a strong foundation for future advancements toward a complete wireless implementation.

II. Impedance Interferometry Sensor

An *impedance interferometry sensor* is introduced, leveraging impedance variations within the roller cavity as a function of temperature (see Fig. 2(a)). These variations arise from changes in the geometry of bimetallic strips strategically positioned within the cavity (see Fig. 2(b) and (c)). Metal 3D printing facilitates the integration of these components into an all-metal environment, which is essential for high temperature sensing requirements exceeding 350°F. This study characterizes the impedance variations of this geometry, which can be extracted using a passive RFID system positioned on the end-cap regions of the roller.

Several temperature-sensing solutions are currently available. The most commonly used are thermocouples [6] and

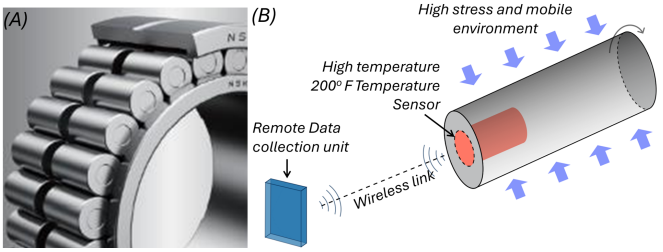

Fig. 1. (a) Bearing containing cylindrical rollers used in high-stress environment such as wind turbines and railroad axles. (b) Concept sketch showing conceptualized system and need for passive RF sensor for high temperature sensing.

resistance temperature detectors (RTDs). However, these are typically oversize and unable to operate effectively in the harsh environment of rotating roller bearings. Their installation and maintenance are also complex and costly. Infrared thermography [7] has also been used, but it primarily measures surface temperatures and cannot accurately detect internal temperatures within the bearing, where overheating often originates. Vibration analysis can indicate bearing faults [8] [9], but it provides only indirect temperature information and may lack the sensitivity required for detecting early-stage overheating. Acoustic Emission (AE) monitoring [10], which is mainly used to detect bearing faults such as cracks, can produce temperature-influenced signals. However, the relationship between AE signals and temperature is complex, making this method unsuitable for precise temperature measurement. Furthermore, oil sampling analysis [11] can provide insight into bearing wear and lubricant degradation, but these methods are time-consuming, particularly in wind turbine applications, and cannot measure real-time temperature changes. In contrast, our proposed RFID-based method offers potential advantages by enabling wireless temperature sensing and facilitating localized temperature measurements.

III. Simulations Modeling and Optimization

To ascertain sufficient variation in the impedance, an Ansys Electronics Desktop Simulation Model was developed using a finite element method (FEM)-based numerical simulation. The model was used to optimize the dimensions and positions of a pair of bimetallic strips, a probing pin, and the surrounding cavity, as shown in Fig. 3.

(1) Roller Design: The roller has a total length of 7.7 cm, an outer radius of 1.65 cm, and an inner hole radius of 0.6 cm. Within the bearing, a cavity measuring 3 cm in length is incorporated.

(2) Coaxial Cable Integration: A copper coaxial cable is inserted into the roller, with the tail section of the cable

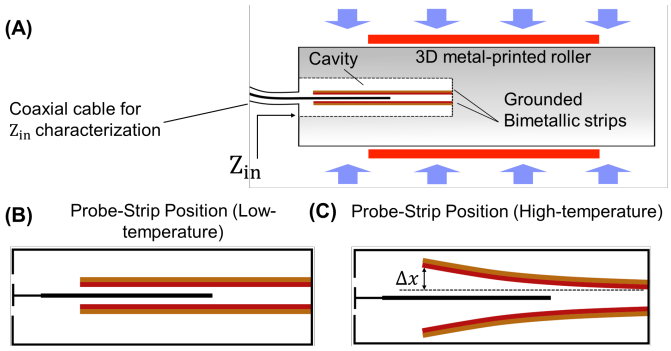

Fig. 2. (a) Sensing set-up used to characterize temperature dependent impedance of the cavity in roller (b) Bimetallic strip positions for low-temperature case (C) Bimetallic strip positions for high-temperature case

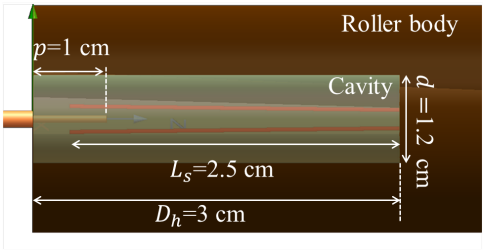

Fig. 3. Simulation model and optimized dimensions of the cavity, probe and bimetallic strips.

stripped to expose the copper conductor. The exposed portion of the copper conductor, which acts as a probe, is 1 cm long. *(3) Bimetallic Strip Inside the Cavity:* A bimetallic strip is placed inside the cavity, consisting of two single strips connected at the base, each 4.6 cm in length, 1 mm in width, and 0.5 mm in thickness. The strip bends in response to thermal stress, with a displacement range varying from 0 mm (no bending) to 3 mm (maximum bending). At around 2 mm bending, the bimetallic strip contacts the roller. When no displacement occurs, the copper conductor is centrally aligned between the two strips.

A wave port for excitation was created and connected to the far end of the coaxial cable. To define the excitation at the coaxial-roller interface, the de-embedding option in the post-processing tab of Ansys software was used to refine the excitation settings. This provided S parameters and impedance values at the roller edge, as would be observed by an integrated RFID.

To simulate the effects of temperature variation, a parametric sweep was performed on the parameter Δx, representing the bending displacements of the tip of the bimetallic strip from 0 mm to 2 mm, with increments of 0.2 mm. The S_{11} plot, along with the corresponding plots for the imaginary (Z_{im}) and real (Z_{real}) components of impedance at the port at 1.6 GHz, was generated. The bending of the bimetallic strip significantly affects the S_{11} parameter only above 1.5 GHz. This provides a useful reference for selecting an optimal frequency in which the changes are monotonic and are more easily analyzed.

Based on the temperature, where a bend displacement of 0 mm corresponds to 70°F and 2 mm corresponds to 400°F, a plot of Z_{im} versus temperature is generated. Since the primary focus is on the impedance of the system, complex S_{11} is used to calculate Z_{11}. The variation of the real and imaginary parts of Z_{11} with bending is shown for 1.6 GHz in Fig. 5. As noted due to capacitive coupling between the signal probe (center conductor) and bimetallic strip, we observe a negative $\Re(Z_{11})$, which shows variation with bend displacement parameter used in the simulations.

IV. Experimental Validation

In order to make this an actual application, we performed a measurement based on the simulation. For this measurement, a stainless steel roller of the simulated dimensions was used with a blank hole on one side. A screwable plug with bimetallic strips was then inserted into the blank hole to produce the geometry shown in the simulations. A coaxial cable with an extended pin is then used to create the required capacitive coupling between the input cable and the bimetallic strips. An electric heater is used to heat the roller for temperature variation tests, and a type J thermocouple is attached to the side of the bearing for temperature measurements.

The characterization set-up and pictures of the roller are shown in Fig. 6. As shown, the center pin of the roller is excited using an RF signal, which is used to measure the reflection coefficient (S_{11}). The roller is then heated with an electric heater which slowly increases the temperature of the metal block. For consistent measurements, the temperature was made to be stable at each data point for a couple of minutes before the measurements were taken. Temperature variations are recorded between 50^o F and 350^o F in steps of 5 - 10^o F.

A temperature change of 350°F induces a structural deformation in the bimetallic strip, resulting in an impedance variation of approximately 100 Ω in the imaginary part of the impedance. This significant change in impedance serves as an effective indicator of temperature variation, highlighting the potential of the system for precise thermal monitoring.

Simulation versus Measurements: We note that qualitatively, the variations in real and imaginary parts of Z_{11} are similar in measurements and simulations. This aids to consistency of sensor operation and its theoretical understanding. The real

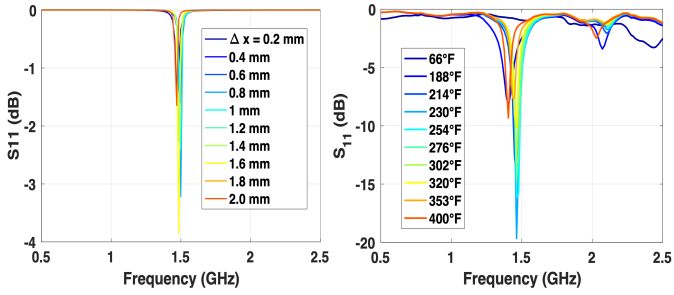

Fig. 4. *Left:* Variation of reflection coefficient S_{11} as a function of tip-displacement modeled in simulations. *Right:* Measured reflection coefficient S_{11} as a rising temperature from heat applied to roller.

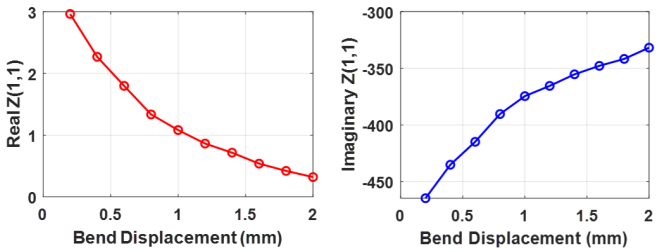

Fig. 5. Simulated variation in input impedance Z_{11} with changing bend position.

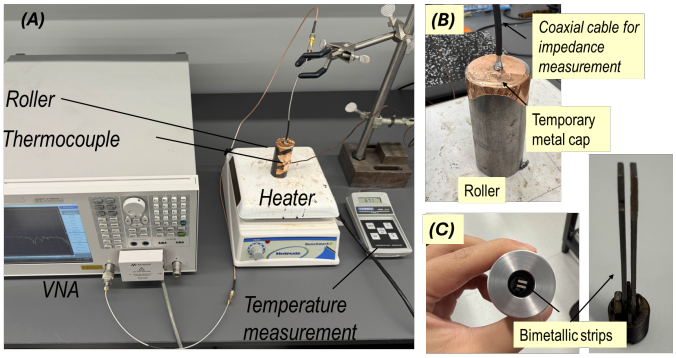

Fig. 6. (a) Measurement set-up (b) Roller and coaxial cable (c) Position of bimetallic strips, top-view.

part of the impedance shows a much stronger variation with heat; however, this could be artifacts of added sources of loss near the resonant frequency of the cavity. We observe an excellent match in the resonance frequency observed in the measured data with simulated data.

Consistency of Measurements: Real and imaginary parts of impedance obtained from the S_{11} data are shown in Fig. 7. As noted, the imaginary part monotonically increases in capacitive regime and the real part monotonically decreases. The measurements were performed 5 times including with horizontal position of the roller. Each time trend is confirmed with reasonable precision in the measurement data.

V. Conclusion

The proposed sensor concept successfully combines the operation of bimetallic strips with impedance variations, as demonstrated through simulation and measurement studies. Due to the use of all-metal parts, the sensor is robust, tolerant to high temperatures and high stress, and integrable with practical metal rollers for various applications. Simulations were conducted using Ansys Electronics Desktop with a passive model and coaxial feeding, which effectively guided the development of the experimental setup.

Experimental measurements were performed using external temperature control and impedance measurements around 1.6 GHz, using the higher range of impedance variation near cavity resonance. Significant impedance changes were observed with temperature variations, demonstrating the potential of this system for the prevention of overheating. Future work will focus on integrating the passive impedance interferometry sensor

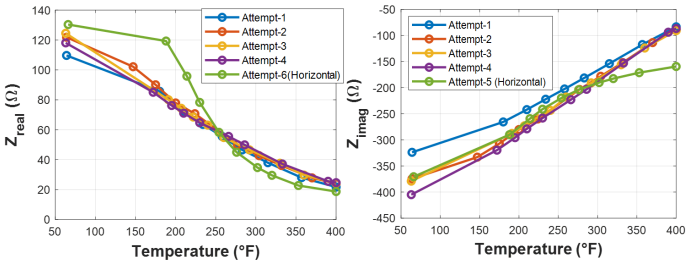

Fig. 7. Measured temperature dependent impedance variation in roller.

with a wireless transceiver or RFID for wireless temperature monitoring.

VI. Future Works

Although impedance changes from roller modifications are promising, implementing coaxial cables in wind turbines is impractical due to challenges such as rotational motion, maintenance complexity, and high installation costs. To overcome these limitations, we are focusing on developing a compact RFID chip capable of withstanding high temperatures and optimizing signal reflection. This wireless solution will provide a robust and cost-effective alternative for reliable impedance monitoring in the demanding operational environment of wind turbines, improving both performance diagnostics and system efficiency.

References

[1] G. Singh, K. Sundaram, and M. Matuonto, "A solution to reduce overheating and increase wind turbine systems availability," *Wind Engineering*, vol. 45, no. 3, pp. 491–504, 2021.

[2] G. Yan, C. Yu, and Y. Bai, "Wind turbine bearing temperature forecasting using a new data-driven ensemble approach," *Machines*, vol. 9, no. 11, 2021. [Online]. Available: https://www.mdpi.com/2075-1702/9/11/248

[3] H. Li, J. Deng, S. Yuan, P. Feng, and D. D. Arachchige, "Monitoring and identifying wind turbine generator bearing faults using deep belief network and ewma control charts," *Frontiers in Energy Research*, vol. 9, p. 799039, 2021.

[4] W. Yang, C. Liu, and D. Jiang, "An unsupervised spatiotemporal graphical modeling approach for wind turbine condition monitoring," *Renewable energy*, vol. 127, pp. 230–241, 2018.

[5] W. Yang, R. Court, and J. Jiang, "Wind turbine condition monitoring by the approach of scada data analysis," *Renewable energy*, vol. 53, pp. 365–376, 2013.

[6] A. Z. Kulganatov, E. V. Solomin, and A. A. Berestinov, "Temperature monitoring of wind turbines: Choosing the optimal method or reliable operation," *2024 International Ural Conference on Electrical Power Engineering (UralCon)*, 2024.

[7] B. Yang, L. Zhang, W. Zhang, and Y. Ai, "Non-destructive testing of wind turbine blades using an infrared thermography: A review," in *2013 International Conference on Materials for Renewable Energy and Environment*, vol. 1, 2013, pp. 407–410.

[8] S. Guan, B. Zhu, P. Cui, H. Shen, and A. Wu, "Experimental investigation and simulation on vibration of wind turbine in cooling system of wind power generation," in *2020 4th International Conference on HVDC (HVDC)*, 2020, pp. 102–106.

[9] C. Liu, D. Jiang, and J. Chen, "Vibration characteristics on a wind turbine rotor using modal and harmonic analysis of fem," in *2010 World Non-Grid-Connected Wind Power and Energy Conference*, 2010, pp. 1–5.

[10] Q. Hongwu, X. Xiaoxue, P. Jincheng, J. Tongli, and G. Weifeng, "Using ae testing method for condition monitoring in wind turbine shaft," in *2015 8th International Conference on Intelligent Networks and Intelligent Systems (ICINIS)*, 2015, pp. 173–176.

[11] Q. Wang, Z. Cao, J. Liu, J. Du, X. Ren, and T. Tong, "Wind turbine gearbox oil health assessment method based on deterioration rate variable weight correction," in *2024 IEEE 4th International Conference on Power, Electronics and Computer Applications (ICPECA)*, 2024, pp. 804–808.